Organic & Biomolecular Chemistry

Cite this: *Org. Biomol. Chem.*, 2011, **9**, 6779

www.rsc.org/obc

PAPER

Reactions of dehydrodiferulates with ammonia†

Ali Azarpira,*[a] Fachuang Lu[a,b] and John Ralph[a,b]

Received 29th April 2011, Accepted 23rd June 2011
DOI: 10.1039/c1ob05677h

Lignocellulosic materials derived from forages and agricultural residues are potential sustainable resources for production of bioethanol or other liquid biofuels. However, the natural recalcitrance of such materials to enzymatic hydrolysis is a major obstacle in their efficient utilization. In grasses, much of the recalcitrance is associated with ferulate cross-linking in the cell wall, *i.e.*, with polysaccharide–polysaccharide cross-linking that results from ferulate dehydrodimerization or with lignin–polysaccharide cross-linking that results from the incorporation of (polysaccharide-bound) ferulates or diferulates into lignin, mainly *via* free-radical coupling reactions. Many pretreatment methods have been developed to address recalcitrance, with ammonia pretreatments in general, and the AFEX (Ammonia Fiber Expansion) process in particular, among the more promising methods. In order to understand the polysaccharide liberating reactions involved in the cleavage of diferulate cell wall cross-links during AFEX pretreatment, reaction products from five esters modeling the major diferulates in grass cell walls treated under AFEX-like conditions were separated and characterized by NMR and HR-MS. Results from this study indicate that, beyond the anticipated amide products, a range of degradation products derive from an array of cleavage and substitution reactions, and reveal various pathways for incorporating ammonia-based nitrogen into biomass.

Introduction

Plants provide substantial renewable sources of polysaccharides that can be used as feedstocks for liquid biofuel production. However, in order to make these natural complexes efficiently accessible to microbes and enzymes it is necessary to use some kind of pretreatment to overcome their natural resistance to deconstruction. A number of different pretreatment methods have been developed. They operate at different pH conditions and temperatures and can address varying degrees of recalcitrance.[1–3] Ammonia-based pretreatments are gaining favor, particularly for grasses. Ammonia Fiber Expansion (AFEX), in particular, is one of the more promising physiochemical pretreatments for lignocellulosic materials having the advantage of retaining the whole biomass without producing the usual array of compounds that inhibit saccharification enzymes or are toxic to fermentation microbes. In the AFEX process, liquid ammonia to biomass loading is (0.3–2) : 1 (w/w) and water to biomass is (0.6–2) : 1 (w/w) at 60–130 °C under pressure (200–400 psi) for 5–30 min.[4–8]

Lignin, one of the most abundant polymers in nature, is present in the cell walls of all plants. It is an amorphous and structurally complex polymer produced by combinatorial oxidative coupling of mainly three monolignols, *i.e.*, *p*-coumaryl (normally only as a minor component), coniferyl and sinapyl alcohols (4-hydroxycinnamyl alcohols with different degrees of methoxylation *ortho* to the phenol). These monolignols generate *p*-hydroxyphenyl (H), guaiacyl (G) and syringyl (S) units in the polymer (Fig. 1). These units are asymmetrically joined to each other and, more importantly, to the growing polymer, or between polymer units, mostly *via* β–O–4-, β–5-, β–β-, 5–5-, and 5–O–4-linkages.[9,10] In grasses, ferulates and diferulates may serve as nucleation or initiation sites for lignification.[11]

All three hydroxycinnamates, *p*-coumarate, ferulate and sinapate (Fig. 1) are associated with cell wall polysaccharides; *p*-coumarate is found mainly acylating lignins, in a form that does not contribute to the recalcitrance.[12] Grasses, in particular, have relatively high levels of ferulate and low levels of *p*-coumarate acylating the primary hemicellulosic polymers, the (glucurono)arabinoxylans.[13–15] In addition to the problem lignin poses to efficient saccharification, much of the recalcitrance in grasses is due to cell wall cross-linking that is mediated by ferulates. Polysaccharide–polysaccharide cross-linking results from ferulate dehydrodimerization in the wall, and lignin–polysaccharide cross-linking results from the incorporation of ferulates and diferulates into the radical cross-coupling polymerization reactions of lignification, with which they are fully compatible.[9,10,16,17] Both cross-linking mechanisms have been shown to affect the rate and/or

[a]*DOE Great Lakes Bioenergy Research Center, University of Wisconsin-Madison, Madison WI 53726, USA. E-mail: azarpira@wisc.edu; Fax: +1 608 265 2904; Tel: +1 608 262 1629*
[b]*Department of Biochemistry and Wisconsin Bioenergy Initiative, University of Wisconsin-Madison, Madison WI 53726, USA. E-mail: fachuanglu@wisc.edu, jralph@wisc.edu; Fax: +1 608 265 2904; Tel: +1 608 890 2429*

† Electronic supplementary information (ESI) available: HPLC chromatograms of crude reaction mixtures, proposed mechanisms for some of the reactions, photograph of the pressure vessel, NMR spectra for isolated compounds and ESI spectra for **2d** and **2e**. See DOI: 10.1039/c1ob05677h

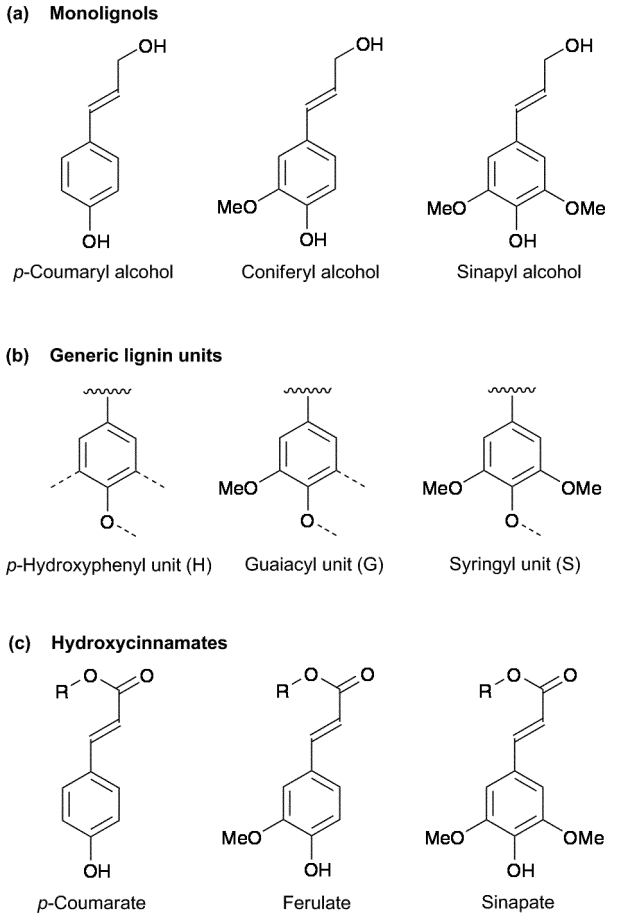

Fig. 1 (a) Primary lignin monomers, (b) generic lignin units, and (c) the hydroxycinnamates.

extent of enzymatic cell wall saccharification.[18] In other words, all of these cross-linking mechanisms between polysaccharides, with each other and with lignin, have a negative impact on the enzymatic bioconversion of cellulose and other wall polysaccharides into fermentable sugars. One of the reasons that AFEX pretreatment works so effectively to improve the digestibility of grasses is that these ferulate (and diferulate) ester bonds are readily cleaved by ammonia, effectively resulting in an efficient destruction of such cross-links, and rendering the polysaccharides more accessible. Cleavage of ferulate ester linkages therefore contributes to the unusually high extractability of grass lignins and the improved enzymatic degradability of grass cell walls after mild alkaline pretreatments.[19] A particular advantage of ammonia-based pretreatments, and AFEX in particular (which retains the entire biomass, without requiring its fractionation), is that nutrients for fermentation are preserved (or even enhanced, due to the increase of N-content) in the biomass.[20]

Utilization of plant derived lignins (or lignin derivatives), which may be generated in significant quantities during pulp and paper making as well as biomass treatment for biofuel production, has been the subject of many studies. Lignin is one of the important substances comprising the organic fraction of soil. Moreover, introduction of nitrogen into lignin using different chemical reactions has drawn special attention due to the successful application of such products as humus-like soil fertilizers.[21,22] Several articles discuss the chemical reactions occurring during the treatment of lignin with ammonia, but the information in this field is limited due to the complex nature of lignin and the possible diverse reactions occurring under different treatment conditions.[22]

To obtain a better understanding of the chemical reactions and structural changes occurring when grass cell walls are treated with ammonia, we studied milligram-scale 'AFEX' pretreatment of models for the important polysaccharide–polysaccharide cross-linking structures, the series of five dehydrodiferulates. Along with anticipated reactions, some rather striking bond-cleavage reactions were observed, which also hint at mechanisms by which macromolecular lignin might be depolymerizing. The reactions of the various dehydrodiferulates are described in this paper.

Results and discussion

Dehydrodiferulates, from here on termed simply diferulates, in the cell wall result from radical coupling of ferulate monomers that acylate wall (glucurono)arabinoxylans. Like lignification reactions, ferulate dehydrodimerization is a combinatorial process, with ferulates coupling with various regiochemistries, giving rise to a series of 5 predominant diferulates (Fig. 2).[9,10,23,24] Although the synthesis of all of these diferulates has been described,[10,23,25] we needed improved methods to generate larger quantities for this and other studies. These dehydrodimers are now available more conveniently from a simpler set of coupling reactions, requiring little in the way of complex organic synthesis. All of the diferulate model compounds were synthesized *via* radical coupling reactions of ethyl or methyl ferulate initiated by the CuCl(OH)–tetramethylethylenediamine complex in acetonitrile or hydrogen peroxide/peroxidase in phosphate buffer as reported elsewhere.[26] All compounds were identical to those previously reported.[23]

From the reaction mixture of ammonia with the acyclic 8–8-diferulate **1** several compounds, in addition to some unreacted compound **1**, were obtained out of which five major products were determined, Scheme 1A. Vanillin **1a** was the simplest product. Compound **1b**, after purification by HPLC, was identified as an oxopyrrolidine derivative. The high resolution electrospray ionization mass spectrometry (HRESIMS) peak for **1b** corresponded with the molecular formula $C_{12}H_{14}N_2NaO_4$. In the ^{13}C NMR spectrum, signals from the 3-methoxy-4-hydroxyphenyl moiety at δ_C 147.6 (C-3), 146.2 (C-4), 132.9 (C-1), 118.4 (C-6), 115.3 (C-5), and 109.9 (C-2) indicated the presence of only one aromatic ring. On the other hand, ^{13}C NMR signals at 60.0 (C-7), 49.3 (C-8), 34.9 (C-8′) and 174.7 (C-9′) along with COSY correlations between δ_H 2.83 (H-8) and 4.60 (H-7) as well as δ_H 2.83 (H-8) with 2.30 (H-8′a) and 2.44 (H-8′b) and HMBC correlations between δ_H 4.60 (H-7), 2.83 (H-8), 2.30 (H-8′a) and 2.44 (H-8′b) with δ_C 174.7 (C-9′) were consistent with a structure containing an oxopyrrolidine ring. HMBC correlations between δ_H 4.60 (H-7) with carbon signals at δ_C 49.3 (C-8), 118.4 (C-6), 109.9 (C-2) and 132.9 (C-1) established the connectivity between the two rings. Compound **1c**, isolated from the reaction mixture of **1**, showed a HRESIMS $(M + Na)^+$ signal corresponding with the molecular formula $C_{20}H_{19}NNaO_7$. ^{13}C NMR signals at δ_C 47.2 (C-8), 179.7 (C-9), 53.8 (C-8′), and 174.6 (C-9′) combined with the HMBC correlation between the doublet proton at δ_H 4.88 (H-8′) with carbon signals at δ_C 47.2 (C-8), 179.7 (C-9) and 174.6 (C-9′) as well as the COSY correlation between proton signals at δ_H 3.46

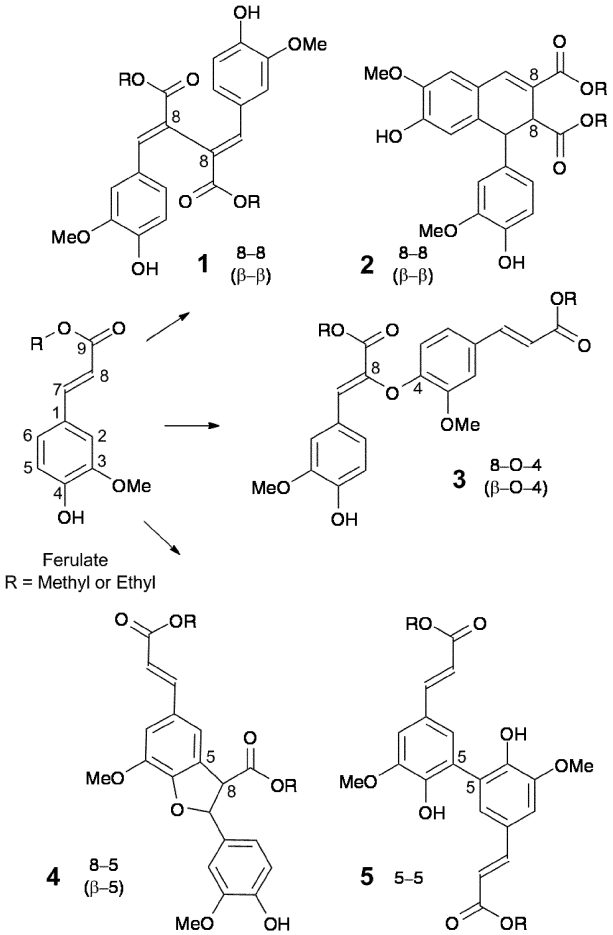

Fig. 2 Diferulates from oxidative coupling of ferulate esters.

(H-8) and 4.88 (H-8′) suggested the presence of the pyrrolidinedione moiety. The HMBC correlations between proton signals at δ_H 2.74 (H-7a) and 3.05 (H-7b) with carbons at δ_C 179.7 (C-9) and 53.8 (C-8′) established the connectivity of the vanillyl moiety and the pyrrolidinedione ring at C-8 while the correlation between δ_H 3.46 (H-8) and 4.88 (H-8′) with δ_C 192.3 (C-7′) established the connection of the second aromatic ring at C-8′. Compound **1d**, obtained as a colorless gum following HPLC purification, was also identified as a pyrrolidinedione derivative. Its HRESIMS peak $(M + Na)^+$ corresponded with the molecular formula $C_{20}H_{20}N_2NaO_6$. The differences between the NMR spectra of **1c** and **1d** were due to the presence of an olefinic double bond substituted with an amino group in **1d**. Simultaneous hydrolysis and aminolysis of compound **1** yielded compound **1e**.

Compounds **2a–2e** (Scheme 1B, Fig. 3) were isolated from the reaction mixture of the cyclic 8–8-diferulate **2**. Compound **2a** was the result of complete aminolysis of the ester **2**. HRESIMS confirmed a molecular formula of $C_{19}H_{17}NNaO_5$ for both **2b** and **2c**. Their ^{13}C NMR spectra indicated the presence of only one carbonyl in the molecule. In the ^1H NMR spectrum of **2b**, the presence of two doublets at δ_H 7.70 (H-7) and δ_H 7.27 (H-8) and their correlation in COSY spectra suggested that the carbonyl moiety is attached to C-8′. This assignment was supported by the 3-bond HMBC correlation between the proton signal at δ_H 7.27 (H-8) and the carbonyl signal at δ_C 171.5 (C-9′). In the ^1H NMR

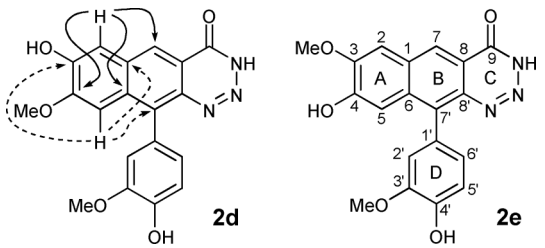

Fig. 3 Proposed structures for compounds **2d** and **2e** and important HMBC correlations.

spectrum of **2c**, the presence of two (broad) singlets at δ_H 8.25 (H-7) and δ_H 7.63 (H-8′) and their correlations with carbonyl signal at δ_C 168.2 (C-9), in the HMBC spectrum, confirmed the presence of the amide carbonyl at C-9, *i.e.*, attached to C8.

A polar fraction obtained from the reaction mixture of cyclic 8–8-diferulate **2** by flash chromatography was purified on HPLC (Luna phenyl-hexyl column) and yielded structural isomers tentatively assigned as **2d** and **2e** (Fig. 3 and 4). The HRESIMS spectrum for **2e** showed a $(M + Na)^+$ peak corresponding with the molecular formula $C_{19}H_{15}N_3NaO_5$. Both compounds showed same ESI $(M + H)^+$ and $(M - H)^-$ peak masses (ESI spectra on pages S45 and S46 in the ESI†). Their NMR data are presented in Table 4. In **2d**, the three-bond HMBC correlation between the proton signal at δ_H 8.13 (H-7) and the carbonyl signal at δ_C 168.8 (C-9) showed the presence of a carbonyl group connected at C-8. Although another HMBC correlation between the proton signal at δ_H 8.13 (H-7) with a carbon signal at δ_C 122.1 (C-8′) was observed, the signal for the C-8 quaternary carbon did not appear in the NMR spectra. The presence of three nitrogen atoms (realized from the MS spectrum) along with the presence of one carbonyl and two quaternary carbons at C-8 and C-8′ (deduced from the NMR spectra) suggested the presence of the ring C. As is observed in Table 4, the main differences in NMR data of **2d** and **2e** are limited to C-2, C-3, C-4 and C-5 (of ring A), whereas the data for rings B, C and D are quite similar. The 2D NMR observations suggested that the methoxyl and hydroxyl group in ring A of **2d** are switched from those in **2e** (Fig. 3). This was deduced from three-bond HMBC correlations in **2d** between the proton signal at δ_H 7.49 (H-2) with carbon signals at δ_C 120.9 (C-7), 130.9 (C-6), and 150.8 (C-4) which showed the presence of the methoxyl group at C-4 of ring A. Also, three-bond HMBC correlations in **2d** between the proton signal at δ_H 7.12 (H-5) with

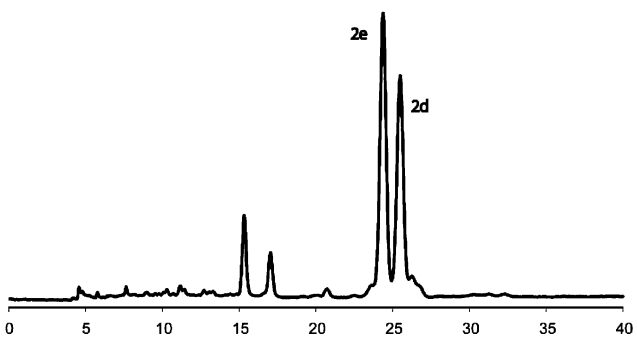

Fig. 4 HPLC profile of the fraction containing **2d** and **2e** (see Experimental section for details).

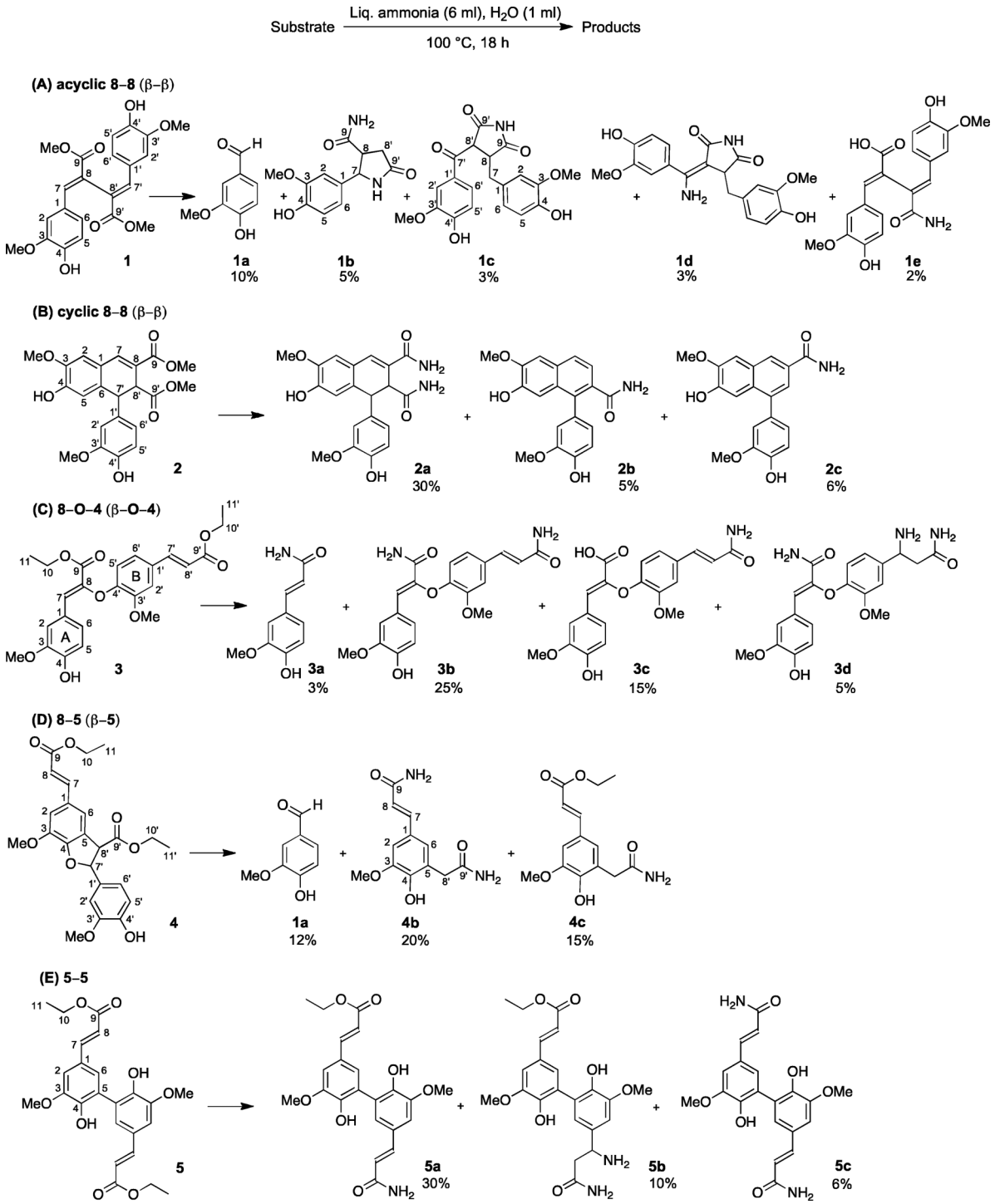

Scheme 1 Reactions of diferulates with liquid ammonia in the presence of water. Isolated yields of the identified products are given.

carbon signals at δ_C 137.8 (C-7′), 131.7 (C-1), and 149.6 (C-3) indicated that the C-3 of ring A was hydroxylated (Fig. 3). In **2e**, on the other hand, three-bond HMBC correlations between the proton signal at δ_H 7.68 (H-2) with carbon signals at δ_C 121.5 (C-7), 130.6 (C-6), and 149.6 (C-4) indicated that the methoxyl group was at C-3 of ring A. Also, three-bond HMBC correlations between the proton signal at δ_H 7.12 (H-5) with carbon signals at δ_C 137.0 (C-7′), 131.5 (C-1), and 150.7 (C-3) further indicated that the hydroxyl group was at C-4 of ring A in **2e**. Currently, we don't have an easy way of explaining the formation of isomer **2d** mechanistically, and the structural assignments for both **2d** and **2e** remain somewhat tentative.

Feruloyl amide (**3a**) was obtained *via* cleavage of the ether bond in the 8–O–4-linked diferulate **3**, Scheme 1C, whereas compounds **3b** and **3c** were more trivially obtained by aminolysis/hydrolysis. The HRESIMS spectrum for **3d** showed an $(M + Na)^+$ peak

Table 1 ^{13}C NMR chemical shift data for compounds[a]

Carbon number	Compounds																
	1a	**1b**	**1c**	**1d**	**1e**	**2a**	**2b**	**2c**	**3a**	**3b**	**3c**	**3d**	**4b**	**4c**	**5a**	**5b**	**5c**
1	127.9	132.9	128.6	127.7	127.5	131.2	128.7	128.2	126.6	123.3	123.5	123.5	123.9	120.9	122.8	118.3	124.7
2	110.4	109.9	112.9	113.1	113.1	112.1	106.5	107.7	111.0	112.7	112.5	112.7	108.9	109.1	108.7	107.6	109.1
3	148.4	147.6	147.3	146.6	147.1	147.2	149.2	149.2	148.3	147.5	147.3	148.1	148.1	148.9	149.0	151.1	147.8
4	154.4	146.2	144.9	144.7	146.7	147.7	147.5	148.7	149.8	148.7	147.7	147.2	148.6	153.3	150.5	159.4	146.3
5	115.5	115.3	115.3	114.8	114.9	116.2	108.6	108.0	116.0	115.5	115.2	115.3	123.5	123.4	126.5	128.3	124.7
6	126.5	118.4	121.1	121.5	123.6	126.4	128.0	128.8	122.1	124.3	124.0	124.1	123.4	125.8	125.8	126.8	123.4
7	190.7	60.0	34.5	33.6	131.9	132.4	125.3	125.7	140.2	122.7	122.4	122.3	139.9	145.7	145.6	146.7	139.6
8	—	49.3	47.2	45.7	136.5	135.0	121.6	128.5	119.3	140.4	140.3	141.1	117.9	111.4	113.2	109.2	118.7
9	—	173.8	179.7	178.8	170.8	169.6	—	168.2	167.6	164.4	164.3	164.6	167.3	166.9	166.8	167.1	167.1
10	—	—	—	—	—	—	—	—	—	—	—	—	—	59.4	59.5	59.1	—
11	—	—	—	—	—	—	—	—	—	—	—	—	—	14.3	14.3	14.2	—
3-OMe	55.5	55.5	55.5	55.8	55.2	55.7	55.5	55.4	55.8	55.0	54.8	54.8	55.6	55.6	55.8	55.2	55.5
1′	—	—	127.4	126.9	127.9	123.1	129.2	131.4	—	129.5	128.9	140.4	—	—	124.0	124.4	124.7
2′	—	—	111.7	115.5	112.2	111.7	114.3	113.8	—	111.0	111.2	110.7	—	—	108.8	109.4	109.1
3′	—	—	147.4	148.5	147.1	146.2	146.9	147.4	—	148.5	148.7	147.3	—	—	148.7	149.6	147.8
4′	—	—	153.5	147.6	146.3	144.9	145.7	146.0	—	146.4	146.9	143.6	—	—	150.5	150.5	146.3
5′	—	—	114.8	111.5	115.0	114.9	115.0	115.4	—	113.2	112.9	112.6	—	—	126.4	128.9	124.7
6′	—	—	124.9	120.8	122.9	119.5	122.4	122.1	—	120.8	121.8	118.0	—	—	123.8	120.7	123.4
7′	—	—	192.3	156.4	131.2	44.8	134.1	137.5	—	138.9	143.5	52.0	—	—	140.1	51.5	139.6
8′	—	34.9	53.8	90.8	133.8	47.4	133.2	123.0	—	120.9	117.5	44.7	37.4	38.1	118.1	39.6	118.7
9′	—	174.7	174.6	178.3	171.8	173.2	171.5	—	—	166.8	167.7	172.7	173.2	173.4	167.3	171.1	167.1
10′	—	—	—	—	—	—	—	—	—	—	—	—	—	—	—	—	—
11′	—	—	—	—	—	—	—	—	—	—	—	—	—	—	—	—	—
3′-OMe	—	—	55.2	55.2	55.3	55.7	55.4	55.6	—	55.6	55.5	55.3	—	—	55.7	55.4	55.5

[a] 125 MHz in DMSO-d_6.

Table 2 ^{1}H NMR data for compounds **1a–1e** and **2a–2c**[a]

Carbon number	Compound							
	1a	**1b**	**1c**	**1d**	**1e**	**2a**	**2b**	**2c**
2	7.34 (s)	6.79 (s)	6.47 (s)	6.24 (s)	7.46 (s)	6.84 (s)	7.32 (s)	7.24 (s)
5	6.93 (d, 8.1)	6.74 (d, 8.1)	6.53 (d, 8.0)	6.52 (d, 7.9)	6.62 (d, 8.3)	6.52 (s)	6.91 (s)	7.39 (s)
6	7.38 (d, 8.1)	6.63 (d, 8.1)	6.57 (d, 8.0)	6.19 (d, 7.9)	6.91 (d, 8.3)	—	—	—
7	9.72 (s)	4.60 (d, 6.8)	H-a: 2.74 (t, 12.5) H-b: 3.05 (dd, 13.8, 4.2)	H-a: 2.64 (d, 11.2) H-b: 2.02 (dd, 13.3, 5.1)	7.03 (s)	7.32 (s)	7.70 (d, 8.2)	8.25 (s)
8	—	2.83 (m)	3.46 (m)	3.86 (s)	—	—	7.27 (d, 8.2)	—
10	—	—	—	—	—	—	—	—
11	—	—	—	—	—	—	—	—
3-OMe	3.81 (s)	3.74 (s)	3.76 (s)	3.81 (s)	3.64 (s)	3.77 (s)	3.73 (s)	3.90 (s)
2′	—	—	7.27 (s)	7.15 (s)	7.22 (s)	6.74 (s)	6.87 (s)	1.98 (d, 1.6)
5′	—	—	6.77 (d, 8.3)	6.91 (d, 8.1)	6.60 (d, 8.3)	6.53 (d, 8.0)	6.84 (d, 7.9)	6.91 (d, 7.9)
6′	—	—	7.35 (d, 8.3)	7.10 (d, 8.1)	6.79 (d, 8.3)	6.21 (d, 8.0)	6.67 (d, 7.9)	6.85 (dd, 7.9, 1.6)
7′	—	—	—	—	7.05 (s)	4.27 (s)	—	—
8′	—	H-a: 2.30 (dd, 16.4, 8.5) H-b: 2.44 (dd, 16.4, 8.5)	4.88 (d, 4.6)	—	—	3.60 (s)	—	7.63 (s)
10′	—	—	—	—	—	—	—	—
11′	—	—	—	—	—	—	—	—
3′-OMe	—	—	3.55 (s)	3.66 (s)	3.68 (s)	3.68 (s)	3.86 (s)	3.81 (s)

[a] 500 MHz in DMSO-d_6, (multiplicity, J in Hz).

corresponding with the molecular formula $C_{20}H_{23}N_3NaO_6$. In **3b**, the NMR spectra showed the presence of an acrylamide side-chain on the B-ring whereas new signals at δ_C 104.4 (C-1′), 52.0 (C-7′), 44.7 (C-8′), and 172.7 (C-9′) in **3d** suggested further ammination of the side-chain. The position of the amino group at C-7′ was confirmed by HMBC correlations between proton signals at δ_H 2.31 (H-8′), 6.77 (H-6′) and 7.12 (H-2′) with the carbon signal at δ_C 52.0 (C-7′) as well as the COSY correlation between protons at δ_H 4.13 (H-7′) with 2.31 (H-8′).

Opening of the tetrahydrofuran ring in the 8–5-linked diferulate **4** yielded vanillin **1a**, with **4b** and **4c** also isolated from the reaction mixture, Scheme 1D. The HRESIMS spectrum for **4b** showed a $(M + Na)^+$ peak corresponding with the molecular formula $C_{12}H_{14}N_2NaO_4$. The NMR spectra of **4b** showed the

Table 3 ^{1}H NMR data for compounds **3a–3d**, **4b**, **4c**, **5a–5c**[a]

Carbon number	Compound								
	3a	**3b**	**3c**	**3d**	**4b**	**4c**	**5a**	**5b**	**5c**
2	7.11 (s)	7.27 (d, 1.7)	7.27 (s)	7.28 (s)	6.99 (d, 1.7)	7.12 (s)	7.27 (s)	7.03 (s)	7.12 (s)
5	6.78 (d, 7.7)	6.74 (d, 8.3)	6.71 (d, 8.2)	6.73 (d, 8.0)	—	—	—	—	—
6	6.97 (d, 7.7)	7.01 (d, 8.3)	7.02 (d, 8.2)	7.03 (d, 8.0)	6.89 (d, 1.7)	6.97 (s)	7.21 (s)	7.16 (s)	6.96 (s)
7	7.30 (d, 15.7)	7.16 (s)	7.15 (s)	7.10 (s)	7.26 (d, 15.7)	7.46 (d, 15.3)	7.56 (d, 15.8)	7.52 (d, 15.5)	7.32 (d, 15.8)
8	6.41 (d, 15.7)	—	—	—	6.37 (d, 15.7)	6.25 (d, 15.3)	6.43 (d, 15.8)	6.20 (d, 15.5)	6.44 (d, 15.8)
10	—	—	—	—	—	4.12, (q, 7.1)	4.15 (q, 7.1)	4.13 (q, 7.1)	—
11	—	—	—	—	—	1.23, (t, 7.1)	1.24 (t, 7.1)	1.23 (t, 7.1)	—
3-OMe	3.79 (s)	3.60 (s)	3.61 (s)	3.59 (s)	3.79 (s)	55.6, (s)	3.82 (s)	3.71 (s)	3.86 (s)
2′	—	7.29 (d, 1.6)	7.45 (s)	7.12 (s)	—	—	7.07 (s)	6.81 (s)	7.12 (s)
5′	—	6.67 (d, 8.3)	6.65 (d, 8.1)	6.57 (d, 8.1)	—	—	—	—	—
6′	—	7.01 (d, 8.3)	7.11 (d, 8.1)	6.77 (d, 8.1)	—	—	7.01 (s)	6.99 (s)	6.96 (s)
7′	—	7.32 (d, 15.8)	7.48 (d, 15.8)	4.13 (s, br)	—	—	7.33 (d, 15.7)	4.43 (t, 6.8)	7.32 (d, 15.8)
8′	—	6.51 (d, 15.8)	6.46 (d, 15.8)	2.31 (d, 4.8)	3.35 (s)	3.31, (s)	6.42 (d, 15.7)	2.68 (d, 6.8)	6.44 (d, 15.8)
10′	—	—	—	—	—	—	—	—	—
11′	—	—	—	—	—	—	—	—	—
3′-OMe	—	3.91 (s)	3.92 (s)	—	—	—	3.38 (s)	3.71 (s)	3.86 (s)

[a] 500 MHz in DMSO-d_6, (multiplicity, J in Hz).

Table 4 ^{1}H NMR[a] and ^{13}C NMR[b] data for compounds **2d** and **2e**

Carbon number	**2d**		**2e**	
	δ_C	δ_H (multiplicity, J in Hz)	δ_C	δ_H (multiplicity, J in Hz)
1	131.7	—	131.5	—
2	112.3	7.49 (s)	109.3	7.68 (s)
3	149.6	—	150.7	—
4	150.8	—	149.6	—
5	106.7	7.12 (s)	110.2	7.12 (s)
6	130.9	—	130.6	—
7	120.9	8.13 (s)	121.5	8.18 (s)
8	X[c]	—	X[c]	—
9	168.8	—	168.9	—
10	—	—	—	—
11	—	—	—	—
Ring A-OMe	55.1	3.69 (s)	55.6	3.93 (s)
1′	125.3	—	125.6	—
2′	114.2	6.97 (s)	114.1	6.89 (s)
3′	146.9	—	146.9	—
4′	146.3	—	146.2	—
5′	115.0	6.89 (d, 8.0)	114.9	6.90 (d, 8.0)
6′	122.6	6.80 (d, 8.0)	122.4	6.73 (d, 8.0)
7′	137.8	—	137.0	—
8′	122.1	—	122.7	—
9′	—	—	—	—
10′	—	—	—	—
11′	—	—	—	—
3′-OMe	55.5	3.74 (s)	55.5	3.74 (s)

[a] 500 MHz in DMSO-d_6, (multiplicity, J in Hz). [b] 125 MHz in DMSO-d_6. [c] Missing carbon signal.

presence of a 5-substituted 4-hydroxy-3-methoxyphenyl moiety. The HMBC correlation between δ_H 7.26 (H-7) with δ_C 108.9 (C-2) and 123.4 (C-6) showed the acrylamide connection at C-1, and correlation between δ_H 3.35 (H-8′) and δ_C 123.4 (C-6), 123.5 (C-5), and 148.6 (C-4) showed the connection of an acetamide moiety at C-5.

Aminolysis/hydrolysis of 5–5-coupled diferulate **5**, Scheme 1E, yielded relatively few compounds, from which **5a**, **5b** and **5c** were isolated and characterized. In **5b**, similarly to in **3d**, ammination of the acrylamide side-chain was observed.

From the outset, we suspected that AFEX pretreatments (or AFEX-like reactions, *e.g.*, ammoniation) are not quite as simple as just cleaving esters and making the corresponding amides.[27] Some esters apparently don't cleave readily, others hydrolyze (rather than being attacked by the nucleophilic ammonia), and some structures undergo more extensive degradation than might be anticipated. Tentative mechanisms have been proposed to show possible pathways leading to the formed products (ESI, Scheme S1†). Phenolic units in lignin are converted into quinone methides at above ~150 °C during the alkaline wood pulping process.[24]

Similarly, all of the diferulate model compounds **1–5**, containing phenolic hydroxyl groups *para* to a conjugated side-chain, can form quinone methide intermediates in basic media; such reactions might be the key steps in the degradation processes (see the ESI†).

Conclusions

There are reports on the analysis of lignocellulosic materials treated with ammonia (in the form of anhydrous ammonia, ammonium hydroxide, or *via* ammoxidation, *etc.*) but their major interest focused on the analysis of nitrogen content in crude product mixtures which enabled these products to be considered as nitrogenous fertilizers.[22,28,29] Comprehensive reports on the isolation and structural elucidation of products from these types of complex reactions are not evident. Here, under conditions similar to those in the AFEX process, diferulates were converted to the expected amides, although acids, amines, and aldehydes were also produced. The survival of some ferulate esters indicated that the AFEX conditions used here might not be optimal for cleaving ferulate esters. Finding nitrogen-containing products other than the expected amides revealed interesting reaction pathways for nitrogen incorporation into the degradation products from grass cell walls and enhance our knowledge of the mechanisms involved in AFEX pretreatment. The carbon–carbon bond cleavage products resulting from 8–5-diferulate, in particular, imply that more complicated reactions than just ester cleavage are involved during the AFEX process. Moreover, results from this study are providing a basis for understanding lignin AFEX reactions that will be further investigated.

Experimental section

General experimental procedures

NMR spectra were acquired on Bruker Biospin (Billerica, MA) AVANCE 500 (500 MHz) spectrometer fitted with a cryogenically cooled 5 mm probe with inverse geometry (proton coils closer to the sample). The central solvent peak was used as reference (DMSO-d_6 δ_H 2.49, δ_C 39.50 ppm). The usual array of ^{1}H, ^{13}C and 2D NMR experiments (gradient-selected COSY, ^{1}H-detected adiabatic 2D-HSQC, and HMBC) were used for structural elucidation of compounds. *J*-values are given in Hz. Conventional lignin numbering was used for carbon numbering. NMR data for all of the compounds are given in Tables 1–4. Ultraviolet-visible (UV-Vis) absorption spectra were recorded on a Shimadzu BioSpec-nano (Shimadzu, Kyoto, Japan) spectrophotometer equipped with a quartz cell adapter. All solvents were HPLC grade and were used as supplied. Flash chromatography was performed on an Isolera One system using SNAP KP-Sil 10 g silica-gel cartridges (Biotage, Dyax Corp., Charlottesville, VA) equipped with a UA-6 UV-vis detector (ISCO, Lincoln, NE). Preparative TLC plates (Analtech TLC Uniplates, 20 × 20 cm coated with 1.5 mm thick silica gel GF with UV 254) were from Newark, DE, USA. Solvents were removed first by rotary evaporator (<50 °C), then further under higher vacuum (100–200 mTorr). HPLC purification and analysis was conducted on a Shimadzu LCMS-2020 (Shimadzu, USA) system comprised of LC-20AD pumps, a SIL-20AC HT autosampler, a CTO-20AC column oven, and using Luna phenylhexyl or Luna C18(2) (250 × 10 mm, 5 µm, Phenomenex, USA) or Kinetex C18 (150 × 4.6 mm, 2.6 µm, Phenomenex, USA) columns at 35 °C. The injection volume was 30–50 µL. Aqueous 0.1% formic acid (v/v, solvent system A) and methanol or acetonitrile (0.1% formic acid, solvent system B) served as the mobile phase in a gradient mode with a flow rate of 2 mL min^{-1}. Detection was at 280 nm *via* a SPD-M20A photodiode array detector. For analysis of the compounds, the following gradient was mostly applied with some modifications for each sample: B from 5 to 30% in 20 min, from 30 to 50% in 5 min, from 50 to 80% in 10 min, and from 80 to 100% in 4 min. Liquid anhydrous ammonia was 99.99% pure. A 16 ml pressure vessel with a multi-port lid (stainless steel grade 316) from HEL Inc. USA was used to perform the AFEX reactions (see the ESI, Fig. S2†).

Typical procedure for AFEX reactions, and purification of products

Anhydrous ammonia gas was liquefied in a liquid nitrogen-cooled conical flask. Note: ammonia gas/liquid is extremely dangerous to health and is chemically corrosive. Caution should be exercised at all times.. To a cooled steel vessel containing a mixture of frozen deionized water (1 mL) and the diferulate model compound (100 mg) was added 6 mL liquid ammonia *via* a cooled graduated glass pipette. The steel vessel was then sealed and heated up to 100 °C (at which temperature the pressure reached ~400 psi) for 18 h in a heating block. After cooling down the vessel in liquid nitrogen, it was opened under the hood, the ammonia allowed to evaporate as it warmed to room temperature, and the products washed out with methanol. The collected methanol solution was evaporated under vacuum. Fractionation by silica-gel flash chromatography (or *via* TLC) of the obtained dark residue using a gradient of hexane/EtOAc 3 : 1 and then EtOAc/MeOH 10 : 1 yielded several fractions which were purified over preparative TLC or reverse-phase HPLC to obtain the compounds shown in Scheme 1. We had difficulty isolating and elucidating all of the compounds from the reaction mixtures—the yields are isolated yields and the mass balance is not complete. See the ESI for HPLC chromatograms of the crude reaction mixtures showing, in some cases, the considerable complexity of the mixtures of products produced, but also identifying the compounds that were isolated and characterized.†

4-Hydroxy-3-methoxybenzaldehyde (vanillin) 1a. 10% isolated yield from diferulate **1** and 12% from diferulate **4**. Colorless gum, UV (λ max MeOH) 229, 277, 307; ESIMS *m/z* $(M - H)^-$ 151; HRESIMS calc. for $C_8H_8O_3$ $(M - H)^-$ 151.0400, found 151.0401.

2-(4-Hydroxy-3-methoxyphenyl)-5-oxopyrrolidine-3-carboxamide 1b. 5% isolated yield from diferulate **1**. Yellow gum, UV (λ max MeOH) 230, 280; ESIMS *m/z* $(M + Na)^+$ 273; HRESIMS calc. for $C_{12}H_{14}N_2NaO_4$ $(M + Na)^+$ 273.0846, found 273.0840.

3-(4-Hydroxy-3-methoxybenzoyl)-4-(4-hydroxy-3-methoxybenzyl)pyrrolidine-2,5-dione 1c. 3% isolated yield from diferulate **1**. Colorless gum, UV (λ max MeOH) 230, 281, 312; ESIMS *m/z* $(M + Na)^+$ 408; HRESIMS calc. for $C_{20}H_{19}NNaO_7$ $(M + Na)^+$ 408.1059, found 408.1057.

(*Z*)-3-[Amino(4-hydroxy-3-methoxyphenyl)methylene]-4-(4-hydroxy-3-methoxybenzyl)pyrrolidine-2,5-dione 1d. 3% isolated yield from diferulate **1**. Colorless gum, UV (λ max MeOH)

288, 318; ESIMS *m/z* (M + Na)$^+$ 407; HRESIMS calc. for $C_{20}H_{20}N_2NaO_6$ (M + Na)$^+$ 407.1214, found 407.1217.

(2*E*,3*E*)-3-Carbamoyl-2-(4-hydroxy-3-methoxybenzylidene)-4-(4-hydroxy-3-methoxyphenyl)but-3-enoic acid 1e. 2% isolated yield from diferulate **1**. Colorless gum, UV (λ max MeOH) 285, 313; ESIMS *m/z* (M + Na)$^+$ 408; HRESIMS calc. for $C_{20}H_{19}NNaO_7$ (M + Na)$^+$ 408.1059, found 408.1055.

7-Hydroxy-1-(4-hydroxy-3-methoxyphenyl)-6-methoxy-1,2-dihydronaphthalene-2,3-dicarboxamide 2a. 30% isolated yield from diferulate **2**. Colorless gum, UV (λ max MeOH) 248, 288; ESIMS *m/z* (M + Na)$^+$ 407; HRESIMS calc. for $C_{20}H_{20}N_2NaO_6$ (M + Na)$^+$ 407.1214, found 407.1214.

7-Hydroxy-1-(4-hydroxy-3-methoxyphenyl)-6-methoxy-2-naphthamide 2b. 5% isolated yield from diferulate **2**. Colorless gum, UV (λ max MeOH) 245, 289; ESIMS *m/z* (M + Na)$^+$ 362; HRESIMS calc. for $C_{19}H_{17}NNaO_5$ (M + Na)$^+$ 362.1004, found 362.1012.

6-Hydroxy-4-(4-hydroxy-3-methoxyphenyl)-7-methoxy-2-naphthamide 2c. 6% isolated yield from diferulate **2**. Colorless gum, UV (λ max MeOH) 251, 310; ESIMS *m/z* (M + Na)$^+$ 362; HRESIMS calc. for $C_{19}H_{17}NNaO_5$ (M + Na)$^+$ 362.1004, found 362.1010.

7-Hydroxy-10-(4-hydroxy-3-methoxyphenyl)-8-methoxy-10,10*a*-dihydronaphtho[2,3-*d*][1,2,3]triazin-4(3*H*)-one 2d. (tentative structural assignment). 2% isolated yield from diferulate **2**. Colorless gum, UV (λ max MeOH) 283; ESIMS for $C_{19}H_{15}N_3O_5$ (M + H)$^+$ found 366 and (M-H)$^-$ found 364.

8-Hydroxy-10-(4-hydroxy-3-methoxyphenyl)-7-methoxy-10,10*a*-dihydronaphtho[2,3-*d*][1,2,3]triazin-4(3*H*)-one 2e. (tentative structural assignment). 2.2% isolated yield from diferulate **2**. Colorless gum, UV (λ max MeOH) 283; ESIMS *m/z* (M+H)$^+$ 366; (M – H)$^-$ found 364; HRESIMS calc. for $C_{19}H_{15}N_3NaO_5$ (M + Na)$^+$ 388.0904, found 388.0910.

(*E*)-3-(4-Hydroxy-3-methoxyphenyl)acrylamide 3a. 3% isolated yield from diferulate **3**. Colorless gum, UV (λ max MeOH) 317, 232; ESIMS *m/z* (M + H)$^+$ 194; HRESIMS calc. for $C_{10}H_{12}NO_3$ (M + H)$^+$ 194.0812, found 194.0818.

(*Z*)-2-(4-((*E*)-3-Amino-3-oxoprop-1-en-1-yl)-2-methoxyphenoxy)-3-(4-hydroxy-3-methoxyphenyl)acrylamide 3b. 23% isolated yield from diferulate **3**. Colorless gum, UV (λ max MeOH) 294, 316; ESIMS *m/z* (M + Na)$^+$ 407; HRESIMS calc. for $C_{20}H_{20}N_2NaO_6$ (M + Na)$^+$ 407.1214, found 407.1207.

(*Z*)-2-{4-[(*E*)-3-Amino-3-oxoprop-1-en-1-yl]-2-methoxyphenoxy}-3-(4-hydroxy-3-methoxyphenyl)acrylic acid 3c. 15% isolated yield from diferulate **3**. Colorless gum, UV (λ max MeOH) 292, 315; ESIMS *m/z* (M + Na)$^+$ 408; HRESIMS calc. for $C_{20}H_{19}NNaO_7$ (M + Na)$^+$ 408.1054, found 408.1060.

(*Z*)-2-(4-(1,3-Diamino-3-oxopropyl)-2-methoxyphenoxy)-3-(4-hydroxy-3-methoxyphenyl)acrylamide 3d. 5% isolated yield from diferulate **3**. Colorless gum, UV (λ max MeOH) 295, 317; ESIMS *m/z* (M + Na)$^+$ 424; HRESIMS calc. for $C_{20}H_{23}N_3NaO_6$ (M + Na)$^+$ 424.1485, found 424.1483.

(*E*)-3-[3-(2-Amino-2-oxoethyl)-4-hydroxy-5-methoxyphenyl]-acrylamide 4b. 20% isolated yield from diferulate **4**. Colorless gum, UV (λ max MeOH) 317; ESIMS *m/z* (M + Na)$^+$ 273; HRESIMS calc. for $C_{12}H_{14}N_2NaO_4$ (M + Na)$^+$ 273.0853, found 273.0846.

(*E*)-Ethyl 3-[3-(2-Amino-2-oxoethyl)-4-hydroxy-5-methoxyphenyl]acrylate 4c. 15% isolated yield from diferulate **4**. Colorless gum, UV (λ max MeOH) 305, 325; ESIMS *m/z* (M + Na)$^+$ 302; HRESIMS calc. for $C_{14}H_{17}NNaO_5$ (M + Na)$^+$ 302.0999, found 302.1004.

(*E*)-Ethyl 3-{5′-[(*E*)-3-amino-3-oxoprop-1-en-1-yl]-2′,6-dihydroxy-3′,5-dimethoxy-[1,1′-biphenyl]-3-yl}acrylate 5a. 30% isolated yield from diferulate **5**. Colorless gum, UV (λ max MeOH) 241, 323; ESIMS *m/z* (M + Na)$^+$ 436; HRESIMS calc. for $C_{22}H_{23}NNaO_7$ (M + Na)$^+$ 436.1372, found 436.1373.

(*E*)-Ethyl 3-[5′-(1,3-diamino-3-oxopropyl)-2′,6-dihydroxy-3′,5-dimethoxy-(1,1′-biphenyl)-3-yl]acrylate 5b. 10% isolated yield from diferulate **5**. Colorless gum, UV (λ max MeOH) 326; ESIMS *m/z* (M + Na)$^+$ 453; HRESIMS calc. for $C_{22}H_{26}N_2NaO_7$ (M + Na)$^+$ 453.1633, found 453.1653.

(2*E*,2′*E*)-3,3′-[6,6′-Dihydroxy-5,5′-dimethoxy-(1,1′-biphenyl)-3,3′-diyl]diacrylamide 5c. 6% isolated yield from diferulate **5**. Colorless gum, UV (λ max MeOH) 239, 320; ESIMS *m/z* (M + Na)$^+$ 407; HRESIMS calc. for $C_{20}H_{20}N_2NaO_6$ (M + Na)$^+$ 407.1219, found 407.1205.

Acknowledgements

This work was funded by the DOE Great Lakes Bioenergy Research Center (DOE BER Office of Science DE-FC02-07ER64494). We thank Hoon Kim (Dept. of Biochemistry, U. Wisconsin-Madison) for discussions regarding the NMR of **2d** and **2e**, and Bruce E. Dale, Shishir P. S. Chundawat, and Venkatesh Balan of the Michigan State University branch of the Great Lakes Bioenergy Research Center for discussions on AFEX and for their collaboration on related projects.

References

1 N. Mosier, C. Wyman, B. Dale, R. Elander, Y. Y. Lee, M. Holtzapple and M. Ladisch, *Bioresour. Technol.*, 2005, **96**, 673–686.
2 A. T. W. M. Hendriks and G. Zeeman, *Bioresour. Technol.*, 2009, **100**, 10–18.
3 D. K. Johnson and R. T. Elander, *Biomass Recalcitrance*, 2008, 436–453.
4 E. Sendich, M. Laser, S. Kim, H. Alizadeh, L. Laureano-Perez, B. Dale and L. Lynd, *Bioresour. Technol.*, 2008, **99**, 8429–8435.
5 F. Teymouri, L. Laureano-Perez, H. Alizadeh and B. E. Dale, *Bioresour. Technol.*, 2005, **96**, 2014–2018.
6 B. Bals, H. Murnen, M. Allen and B. Dale, *Anim. Feed Sci. Technol.*, 2010, **155**, 147–155.
7 V. Balan, L. D. Sousa, S. P. S. Chundawat, D. Marshall, L. N. Sharma, C. K. Chambliss and B. E. Dale, *Biotechnol. Prog.*, 2009, **25**, 365–375.
8 S. P. S. Chundawat, B. S. Donohoe, L. D. Sousa, T. Elder, U. P. Agarwal, F. C. Lu, J. Ralph, M. E. Himmel, V. Balan and B. E. Dale, *Energy Environ. Sci.*, 2011, **4**, 973–984.
9 J. Ralph, *Phytochem. Rev.*, 2010, **9**, 65–83.
10 J. Ralph, M. Bunzel, J. M. Marita, R. D. Hatfield, F. Lu, H. Kim, P. F. Schatz, J. H. Grabber and H. Steinhart, *Phytochem. Rev.*, 2004, **3**, 79–96.
11 J. Ralph, J. H. Grabber and R. D. Hatfield, *Carbohydr. Res.*, 1995, **275**, 167–178.

12 J. Ralph, R. D. Hatfield, S. Quideau, R. F. Helm, J. H. Grabber and H. J. G. Jung, *J. Am. Chem. Soc.*, 1994, **116**, 9448–9456.
13 E. Sjöestrom, *Wood Chemistry: Fundamentals and Applications,*, 2nd edn, 1993.
14 M. M. D. Buanafina, *Mol. Plant*, 2009, **2**, 861–872.
15 T. Koshijima and T. Watanabe, *Association Between Lignin and Carbohydrates in Wood and Other Plant Tissues*, 2003.
16 J. Ralph, R. D. Hatfield, J. H. Grabber, H.-J. G. Jung, S. Quideau and R. F. Helm, *ACS Symp. Ser.*, 1998, **697**, 209–236.
17 J. Ralph and R. F. Helm, *Forage Cell Wall Struct. Dig., Int. Symp.*, 1993, 201–246.
18 J. H. Grabber, R. D. Hatfield, F. C. Lu and J. Ralph, *Biomacromolecules*, 2008, **9**, 2510–2516.
19 M. Baucher, C. Halpin, M. Petit-Conil and W. Boerjan, *Crit. Rev. Biochem. Mol. Biol.*, 2003, **38**, 305–350.
20 M. W. Lau and B. E. Dale, *Proc. Natl. Acad. Sci. U. S. A.*, 2009, **106**, 1368–1373.
21 F. Ramirez, V. Gonzalez, M. Crespo, D. Meier, O. Faix and V. Zuniga, *Bioresour. Technol.*, 1997, **61**, 43–46.
22 K. Fischer and R. Schiene, *Chemical Modification, Properties, and Usage of Lignin*, 2002, 167–198.
23 J. Ralph, S. Quideau, J. H. Grabber and R. D. Hatfield, *J. Chem. Soc., Perkin Trans. 1*, 1994, 3485–3498.
24 J. Ralph, G. Brunow, P. J. Harris, R. A. Dixon, P. F. Schatz and W. Boerjan, in *Recent Advances in Polyphenol Research*, vol 1, ed. F. Daayf, A. El Hadrami, L. Adam and G. M. Ballance, Wiley-Blackwell Publishing, Oxford, UK, 2008, vol. 1, pp. 36-66.
25 J. Ralph, M. T. Garcia-Conesa and G. Williamson, *J. Agric. Food Chem.*, 1998, **46**, 2531–2532.
26 F. Lu, L. Wei, A. Azarpira and J. Ralph, submitted, 2011.
27 A. U. Buranov and G. Mazza, *Ind. Crops Prod.*, 2008, **28**, 237–259.
28 D. Meier, V. Zuniga-Partida, F. Ramirez-Cano, N.-C. Hahn and O. Faix, *Bioresour. Technol.*, 1994, **49**, 121–128.
29 A. Potthast, R. Schiene and K. Fischer, *Holzforschung*, 1996, **50**, 554–562.